Proceedings of the 9th International Conference on Aluminium Alloys (2004)
Edited by J.F. Nie, A.J. Morton and B.C. Muddle

Plastic Anisotropy in Recrystallized and Unrecrystallized Extruded Aluminium Profiles

Ø. Ryen[1], B. Holmedal[1], S. Li[2], P. Van Houtte[3], H.J. Roven[1], E. Nes[1]

[1] Department of Materials Technology, Norwegian University of Science and Technology, N-7491 Trondheim, Norway
[2] Los Alamos National Laboratory, Los Alamos, NM 87545, USA
[3] Department of Metallurgy and Materials Engineering, Katholieke Universiteit Leuven, B-3001 Leuven, Belgium

Keywords: Anisotropy, extruded profiles, texture, Taylor model, EBSD

Abstract

The plastic anisotropy of two recrystallized and two unrecrystallized extruded profiles is analysed. Tensile tests in the solutionised condition show strong directionality of properties. The texture is very strong and changes slightly during deformation. The stress-strain curves are corrected by the Taylor factor, calculated from the texture measurements. This gives critical resolved shear stress as a function of resolved shear strain. Assuming that the texture is responsible for all the anisotropy, the shear stress-strain curves in the various directions should coincide. This is partly true for the unrecrystallized alloys but not for recrystallized alloys. This is thought to be related to variations in slip activity in cube grains.

1. Introduction

The formability of a material is defined as its ability to withstand plastic deformation without failure. The ability to be formed into various geometrical shapes is one of the most important properties of aluminium alloys, and some of the properties of interest are the yield strength, the ultimate tensile strength, limit strains and the plastic strain ratio (*r*-value). A material that is isotropic has equal mechanical properties in all directions. Most metals used for practical applications, however, exhibit different properties in different spatial directions. In extruded profiles which have a strong texture, the properties in the profile plane usually vary with the direction of deformation relative to the extrusion direction, and the formability depends on the orientation of the profile in the forming process. Hence, a good understanding of the directionality of properties is necessary in order to improve and optimise forming operations. Several factors are responsible for the anisotropy of mechanical properties. Texture is often considered as the most important contribution, but also the grain shape, precipitates and dislocation structures may influence the properties.

Heat-treatable aluminium alloys, such as those belonging to the AA6xxx and AA7xxx alloy families, get their strength mainly from precipitate particles. These alloys are first solution heat-treated, i.e. heated to the single-phase area of the phase diagram where all alloying elements are dissolved into solid solution. A rapid quench freezes the atoms in a supersaturated solid solution from where the precipitation sequence starts. The precipitation often occurs at room temperature (natural ageing), but in this work the alloys are investigated in the solution heat-treated condition (W-condition). Industrial forming operations are often carried out in this low-strength condition.

2. Experiments

Four industrially significant alloys are investigated: AA6063, AA6082, AA7108 and AA7108*, where the latter alloy is an AA7108 alloy without Zr. The alloys, with composition and heat-treatment given in table 1, were DC-cast and homogenised. Billets with diameter 203 mm were extruded into flat profiles of thickness 3 mm and width 205 mm. Before the tensile tests the specimens were solution heat-treated (SHT) in salt bath for 30 minutes followed by quenching. The subsequent room temperature ageing behaviour was explored by measuring the hardness after various storage times after quenching (figure 1).

Table 1: Chemical composition (wt%) and homogenisation and solution heat-treatment temperatures (°C) of the investigated alloys.

Alloy	Mg	Si	Zn	Mn	Zr	Fe	Cu	Hom. temp.	SHT temp.
AA6063	0.46	0.44	-	0.03	-	0.19	0.006	585	530
AA6082	0.67	1.04	-	0.54	-	0.20	0.003	530	530
AA7108*	0.85	0.05	5.63	0.01	0.001	0.12	0.006	450	480
AA7108	0.74	0.05	4.94	0.03	0.145	0.14	0.005	450	480

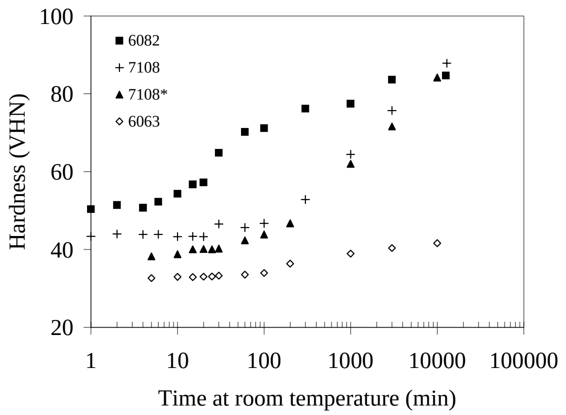

Figure 1: Ageing behaviour at room temperature.

The tensile specimens were cut from the extruded profiles in different directions with respect to the extrusion direction: 0°(ED), 45° and 90° (TD). The tensile testing was performed in the W-temper (max 3 min after SHT) in order to avoid any effects from natural ageing on the test results. A constant crosshead displacement rate corresponding to an initial strain rate of 0.008 /s was used. The specimens had a thickness of 3 mm, a width of 12.7 mm and a parallel length of 65 mm. The test procedure was chosen in accordance with Fjeldly and Roven [1].

Global texture measurements were performed on the normal plane at several positions through the profile thickness. The position is given by s-values, where s=0 represents the mid-thickness and s=1 the profile surface. Additional texture measurements were performed at s=0 before and after tensile deformation. A software was applied to the texture measurements in order to calculate the Taylor factor (*M*) according to the Taylor full constraints (FC) model [2]. The microstructure of the extruded material, as well as the deformation structure after 8% tensile deformation in the 0° and 90° directions of AA7108* were studied using EBSD.

3. Results and Discussion

Based on the microstructure and texture, the alloys investigated in this work can be divided into two groups: Recrystallized and unrecrystallized. The textures are generally very strong, but common for all the alloys is that the surface layer has a weak recrystallized shear texture, also in the unrecrystallized alloys. The fully recrystallized alloys, AA6063 and AA7108*, have equiaxed grains and typical recrystallisation textures, where the main components are cube, ED-rotated cube and Goss in s=0-0.8. AA6063 has considerable texture gradients through the thickness, corresponding to the observation of very coarse grains of Goss-orientation at s=0.5-0.8. AA7108* has a more uniform texture and microstructure than AA6063. The unrecrystallized alloys, AA6082 and AA7108, have a fibrous grain structure with elongated subgrains (δ_{av}≈3 µm) in s=0-0.9. They have a rolling-type texture with dominance of Brass (B), and especially around s=0.75 the B-component is strong. In AA6082 a considerable fraction of coarse cube bands is present in s=0-0.5. The textures at mid-thickness (s=0) of the different alloys are shown in figure 2.

True stress as a function of true plastic strain is plotted for each alloy in figure 3 with the tensile direction at 0°, 45° and 90° with respect to the extrusion direction. Considerable anisotropy is seen in terms of yield strength, work hardening rate and ductility. All the alloys have a low uniform strain in the extrusion direction, while the 45-60° directions appear to the most ductile.

The Taylor factor (FC) is calculated from the texture measurements at mid-thickness before and after tensile deformation and plotted in figure 4. The uniform elongation of the different test directions and alloys varies, so the texture after deformation is measured at strains between 0.12 and 0.28. The most significant changes in the Taylor factor are seen in the 45° of the recrystallized alloys, AA6063 and AA7108*, relating to the unstability of the cube orientation in this tensile direction. In 0° and 90° the cube is stable and exhibit just minor changes. In AA6082, M increases in 0° and decreases in 45°, while in AA7108 a small increase is observed in 0° and 90°.

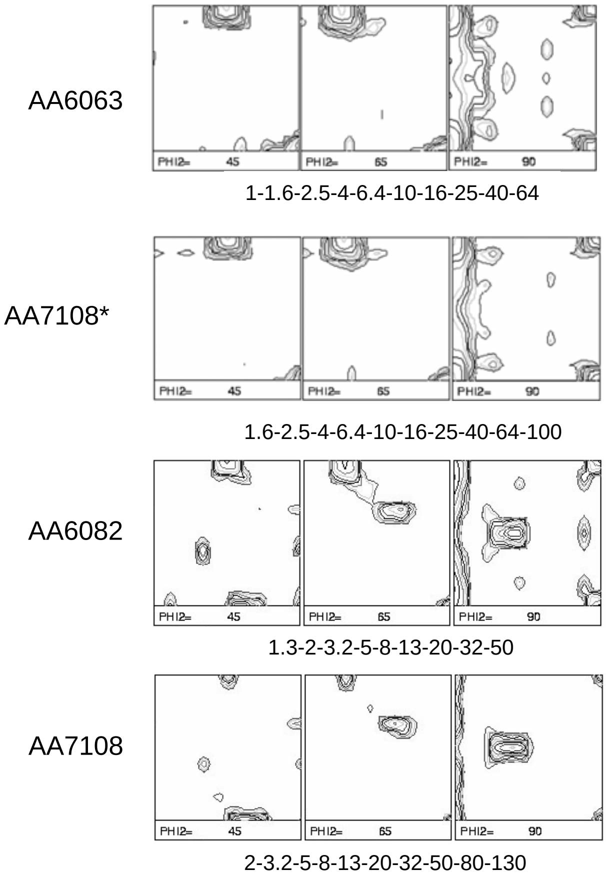

Figure 2: Texture from mid-thickness of the extruded profile (φ_2-sections 45, 65 and 90°).

In figure 4 the Taylor factor is shown as $M=M(\varepsilon)$. Only two points are available for each test direction, but a linear relationship is assumed to be realistic. This is supported by a work on a cube textured AA1200 alloy [3], where the Taylor factor was calculated at ε=0, 0.27 and 0.40, giving a linear evolution of M with ε. We can therefore expect that:

$$\tau = \frac{\sigma}{M(0) + a \cdot \varepsilon} \tag{1}$$

and

$$\gamma = \varepsilon \cdot (M(0) + a \cdot \varepsilon) \tag{2}$$

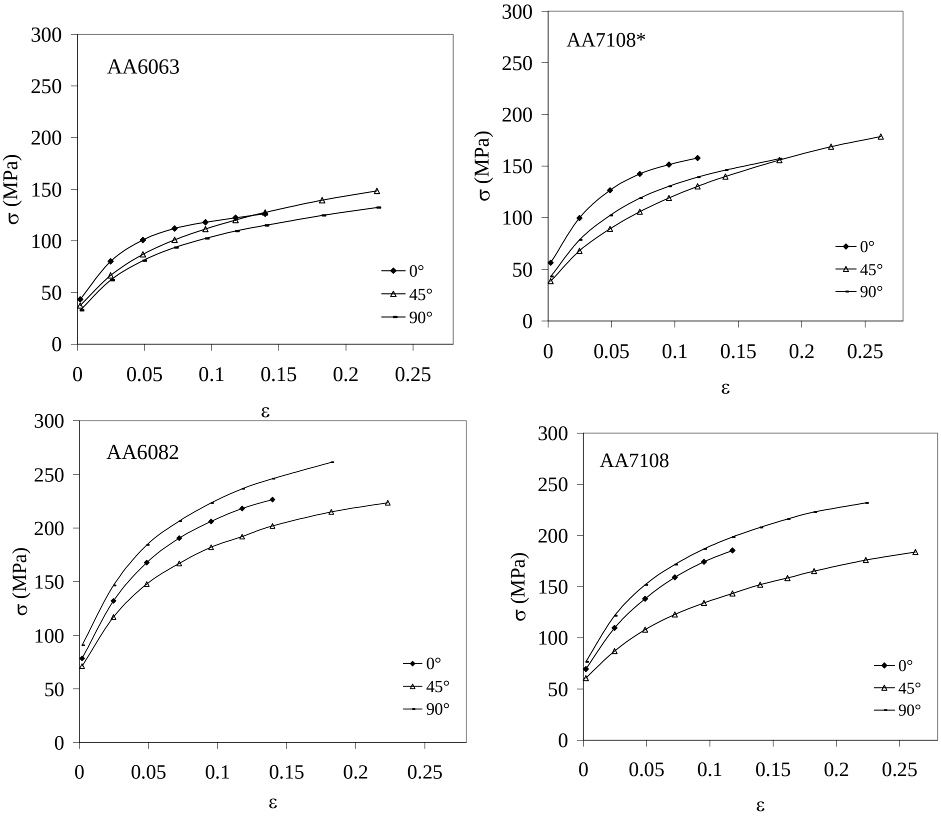

Figure 3: True stress-true strain curves in 0°, 45° and 90° direction of all alloys.

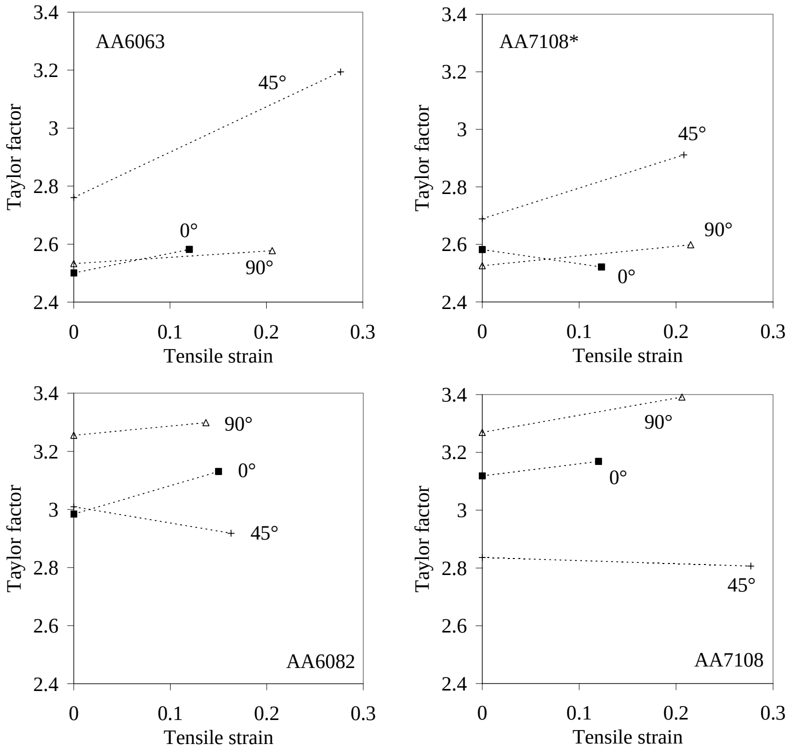

Figure 4: Change in Taylor factor (FC) based on texture measurements before and after tensile deformation in the 0°, 45° and 90°-directions. (a) AA6063 (b) AA7108* (c) AA6082 (d) AA7108.

where *a* is the slope of the dotted lines in figure 4. Using eqs. (1) and (2) a correction for the Taylor factor can be applied to each stress-strain curve, giving shear stress vs. shear strain where the effect of the texture is eliminated. Ideally, if the texture is responsible for the mechanical anisotropy alone, the τ-γ curves should coincide in all test directions. In figure 5 the τ-γ curves are shown for the 0°, 45° and 90° directions of the four alloys.

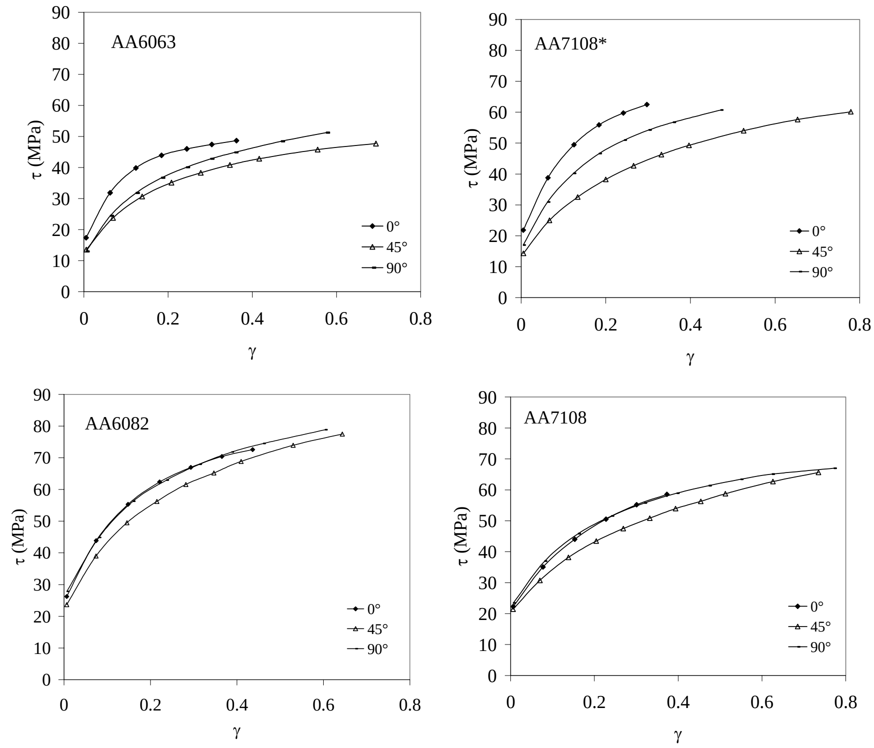

Figure 5: Curves showing shear stress vs. shear strain (τ-γ) for three directions of each alloy, estimated by correcting for the Taylor factor calculated before and after tensile deformation.

Considering the recrystallized alloys first, the correction for the *M*-value (figure 5) has not managed to get the τ-γ curves any closer together, compared to the σ-ε curves in figure 3. In fact, the 45°-curves of the two alloys are even further away from the other. Other authors, who have investigated cube textured alloys, have reported equal stress-strain behaviour for the 0° and 90°-directions because the Taylor factor is equal for cube grains tested in these directions [4,5]. The present alloys do, indeed, have a *rotated* cube texture (figure 2). This may cause a different Taylor factor between 0° and 90°, but it is difficult to believe that this is sufficient. It should be noted that the textures we are working with here are so strong that the software used for calculations of texture and Taylor factors may have problems with the discretisation of the ODF. A finer resolution than the 5°x5°x5° discretisation used here would be preferable. On the other hand, the software has been shown to calculate the *r*-values (*r*=width strain/thickness strain) in excellent agreement with experiments [6]. Another factor causing the anisotropy may possibly lie in a different slip activity in cube grains depending on the test direction. This is indicated by a different evolution of sub-structure whether the material is tensile tested in the 0° or the 90° direction, figure 6. In 0° a tendency of alignment is observed in some grains, whereas in 90° a more evenly distributed dislocation structure is apparent. This is consistent with an observation of rapidly developing microband structures in the 0°-direction of an AA7030 alloy [7] and may suggest that in the 0°-direction slip is restricted to just a few slip systems, leading to a clustering of microbands on the {111}-planes.

The concentrated slip activity will give a strong hardening on the active slip systems, and may explain the strong work hardening in the 0°-direction of AA6063 and AA7108*.

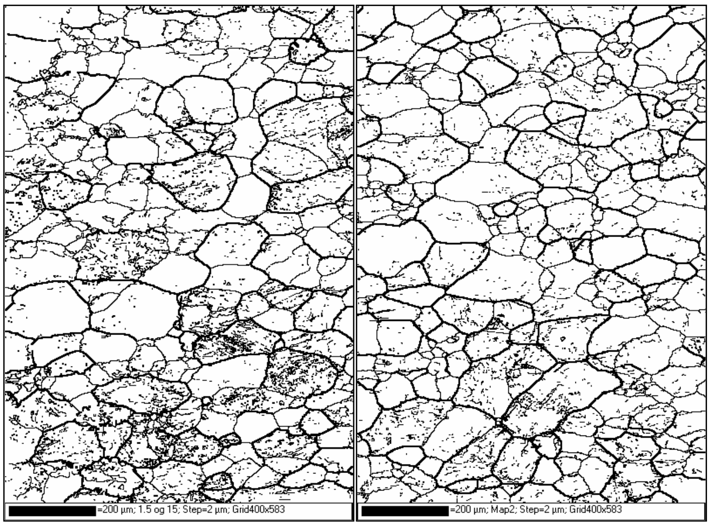

(a) (b)

Figure 6: EBSD maps showing grain boundaries (thick, >15°) and sub-boundaries (thin, >1.5°) of AA7108*. (a) 8% tensile deformation in 0° direction. (b) 8% tensile deformation in 90° direction.

The Taylor factor correction of the unrecrystallized alloys gives more promising results. It is seen that the differences between the σ-ε curves in figure 3 are relatively large. After correcting for the Taylor factor the 0° and 90° τ-γ curves coincide, figure 5. At the yield point all the three directions have nearly identical shear stresses, while the 45°-direction lies a bit below at intermediate strains. The latter is not surprising as the work hardening rates are similar for 0° and 90°, but significantly lower for 45°.

These results demonstrate that the Taylor FC model is useful for predicting the mechanical anisotropy of materials with a fibrous structure and a strong rolling-type texture. They also indicate that the texture is the main contributor to anisotropy in these alloys. Some deviations arise when a different work hardening behaviour comes into account, as for the 45°-direction. The effect of work hardening is obviously a problem for the Taylor model, and this is especially evident in the recrystallized alloys, which have large differences in the work hardening rate. An integration of a work hardening model with the Taylor model is in progress [8].

Acknowledments

This research was carried out as part of the EC Fifth Framework project VIRFORM, Contract No. G1RD-CT-1999-00155. Funding by the European Community and by the industrial partners is gratefully acknowledged.

References

[1] A. Fjeldly, H.J. Roven, Metall. Mater. Trans., 31A, 669-678, 2000.
[2] P. Van Houtte, The “MTM-FHM” software system, version 2, manual, Katholieke Universiteit Leuven, Belgium, 2000.
[3] P. Bate, E. Eardley, F.J. Humphreys, unpublished work, 2002.
[4] A.B. Lopes, F. Barlat, J.J. Gracio, J.F. Ferreira Duarte, E.F. Rauch, Int. J. Plasticity, 19, 1-22 , 2003.
[5] F. Li, P. Bate, Acta Metall. Mater., 39, 2639-2650, 1991.
[6] Ø.Ryen, PhD thesis, NTNU, 2003.
[7] A. Søreng, PhD thesis, NTNU, 1997.
[8] B. Holmedal, Ø. Ryen, P. Van Houtte, E. Nes, Aluminium, 78, 923-926, 2002.